

# Complete $T_c$ suppression and Néel triplets-mediated exchange in antiferromagnet-superconductor-antiferromagnet trilayers

Lina Johnsen Kamra,<sup>1,2,\*</sup> Simran Chourasia,<sup>2,\*</sup> G. A. Bobkov,<sup>3</sup>  
V. M. Gordeeva,<sup>3</sup> I. V. Bobkova,<sup>3,4</sup> and Akashdeep Kamra<sup>2</sup>

<sup>1</sup>*Center for Quantum Spintronics, Department of Physics,  
Norwegian University of Science and Technology, NO-7491 Trondheim, Norway*

<sup>2</sup>*Condensed Matter Physics Center (IFIMAC) and Departamento de Física Teórica de la Materia Condensada,  
Universidad Autónoma de Madrid, E-28049 Madrid, Spain*

<sup>3</sup>*Moscow Institute of Physics and Technology, Dolgoprudny, 141700 Moscow, Russia*

<sup>4</sup>*National Research University Higher School of Economics, Moscow, 101000 Russia*

An antiferromagnetic insulator (AFI) bearing a compensated interface to an adjacent conventional superconductor (S) has recently been predicted to generate Néel triplet Cooper pairs, whose amplitude alternates sign in space. Here, we theoretically demonstrate that such Néel triplets enable control of the superconducting critical temperature in an S layer via the angle between the Néel vectors of two enclosing AFI layers. This angle dependence changes sign with the number of S monolayers providing a distinct signature of the Néel triplets. Furthermore, we show that the latter mediate a similarly distinct exchange interaction between the two AFIs' Néel vectors.

## I. INTRODUCTION

Hybrids comprising a conventional spin-singlet superconductor (S) and one or more magnetic layers realize unconventional superconductivity and Cooper pairs thereby enabling intriguing physics and potential applications [1–7]. The central role of magnets in this engineering of superconductivity is to induce a spin-splitting field which generates spin-triplet Cooper pairs from their spin-singlet counterparts available in S [8–10]. This also reduces the superconducting critical temperature  $T_c$ . A canonical structure sandwiches a thin S layer between two ferromagnet (F) layers and enables a control over the  $T_c$  via the relative angle  $\alpha$  between the two F magnetizations [11–19]. The dominant effect in this trilayer is the addition (cancellation) of spin-splitting fields from the two Fs when their magnetizations are parallel (antiparallel) resulting in the smallest (largest)  $T_c$  out of all F configurations. This has been exploited to switch the S to its normal resistive state by controlling  $\alpha$  via an applied magnetic field. This in turn admits a change of resistance from zero to a nonzero value i.e., an infinite magnetoresistance [13, 18, 19].

The dipolar stray fields and GHz frequency magnons in F are parasitic detrimental influences in these devices. Employing antiferromagnets (AFs) could significantly reduce these problems due to their zero net magnetization and higher magnon frequencies [20–23]. Furthermore, their two or more sublattices admit intriguing phenomena that bring along entirely novel functionalities [24]. However, early experiments with metallic AFs found no influence on an adjacent S, attributing this to their lack of net magnetization and thus spin-splitting field [25]. Subsequently, there have been theoretical predictions of

spin-dependent transport at such AF–S interfaces [26–29]. More recent experiments find a strong effect of the AF on an adjacent S layer [30–35]. An AF or antiferromagnetic insulator (AFI) bearing an uncompensated interface to the adjacent S has recently been shown to induce spin-splitting [23], which contributes to influencing the S.

Intriguingly and subsequently, even a compensated interface with an AFI [Fig. 1(a)] was found to be spin-active [36]. This has recently been understood as being due to the generation of the so-called Néel triplet Cooper pairs [37]. These have been so named as their amplitude changes sign from one lattice site to the next [Fig. 1(b)], while the magnitude varies slower on the coherence length scale. This alternation of sign is due to the Néel triplets being formed from interband pairing [37]. Alternately, within an extended Brillouin zone scheme, they can be considered to result from finite-momentum pairing. In contrast, the regular spin-triplet Cooper pairs generated by an adjacent F only manifest a gradual spatial variation at the coherence length scale associated with the usual intraband pairing [2, 3].

In this Article, we theoretically investigate how such Néel triplet Cooper pairs enable intriguing phenomena in an AFI–S–AFI trilayer [Fig. 1(a)]. Employing the Bogoliubov–de Gennes framework, we show that the critical temperature of the S layer depends on the angle  $\theta$  between the two AFIs' Néel vectors via a dominant  $\cos \theta$  variation and a weaker  $\sin^2 \theta$  contribution. The dominant effect is due to the constructive [Fig. 1(c)] or destructive [Fig. 1(d)] interference between the Néel triplets generated by the two AFI–S interfaces [37], while the  $\sin^2 \theta$  term is reminiscent of equal-spin triplets resulting from noncollinearity between the two Néel vectors [38–41]. For large enough AFI–S interfacial exchange coupling, a complete and abrupt suppression of superconductivity (i.e.,  $T_c \rightarrow 0$ ) is achieved. Due to the alternating sign of Néel triplet correlations, the  $T_c$  vs.  $\theta$  dependence reverses

\* These two authors contributed equally.

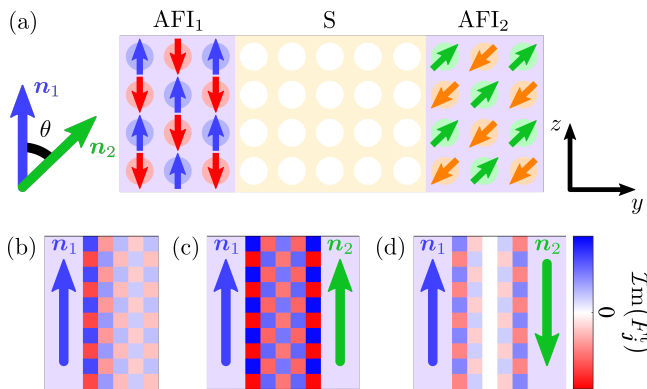


FIG. 1. Schematic depiction of the system and key underlying phenomena. (a) A conventional superconductor (S) is sandwiched between two compensated antiferromagnetic insulators (AFIs) bearing Néel vectors  $\mathbf{n}_1$  and  $\mathbf{n}_2$  that subtend an angle  $\theta$ . (b) In an AFI-S bilayer, spatially alternating spin-splitting induced by the AFI predominantly generates Néel spin-triplet Cooper pairs characterized by a checkerboard pattern of their amplitude  $F_j^z$  [37] thus manifesting an alternating spatial parity. (c) In an AFI-S-AFI trilayer with odd number (considered 5 here) of S monolayers and  $\theta = 0$ , the Néel triplets generated by the two AFIs interfere constructively. This results in more induced spin-triplets and larger weakening of the spin-singlet superconductivity. (d) If instead  $\theta = \pi$ , the Néel triplets from the two AFI-S interfaces interfere destructively and superconductivity is weakened less. This dependence of the superconducting state on  $\theta$  is reversed when the number of S monolayers is even due to the checkerboard pattern associated with the Néel triplets.

when the number of S monolayers changes parity providing a distinct and unique signature of the Néel triplets' role. By computing the superconducting free energy density as a function of  $\theta$ , we further demonstrate that the generated Néel Cooper pairs mediate coupling between the two AFIs' Néel vectors exhibiting the signature parity effect with the S monolayers number. Our theoretical results suggest a direct experimental probe of these recently predicted Néel triplets [37] while enabling antiferromagnetic superconducting spintronics devices.

## II. SYSTEM AND THEORETICAL MODEL

We consider a thin-film superconductor which on each side is interfacing an antiferromagnetic insulator, as schematically depicted in Fig. 1(a). While electron hopping is only allowed within the S layer, the two AFIs impose a local spin-splitting via interfacial exchange onto the atomic layer closest to the S-AFI interfaces [23, 37].

We can thus describe the system by the Hamiltonian

$$H = -t \sum_{\langle i,j \rangle, \sigma} c_{i,\sigma}^\dagger c_{j,\sigma} - \mu \sum_{j,\sigma} c_{j,\sigma}^\dagger c_{j,\sigma} - \frac{J}{2} \sum_j \mathbf{M}_j \cdot \mathbf{S}_j + \sum_j \left( \frac{|\Delta_j|^2}{U} + \Delta_j^* c_{j,\downarrow} c_{j,\uparrow} + \Delta_j c_{j,\uparrow}^\dagger c_{j,\downarrow}^\dagger \right). \quad (1)$$

Here,  $c_{j,\sigma}^{(\dagger)}$  is the annihilation (creation) operator associated with an electron of spin  $\sigma$  at lattice site  $\mathbf{j} \equiv (j_z, j_y)$ ,  $t$  parametrizes electron hopping between nearest neighbor sites within the S,  $\mathbf{S}_j \equiv \sum_{\sigma,\sigma'} c_{j,\sigma}^\dagger \boldsymbol{\sigma}_{\sigma,\sigma'} c_{j,\sigma'}$  is the spin operator for S electrons with  $\boldsymbol{\sigma}$  as the vector of Pauli matrices, and  $\Delta_j \equiv -U \langle c_{j,\downarrow} c_{j,\uparrow} \rangle$  is the self-consistently evaluated mean-field superconducting gap [42]. The chemical potential  $\mu$  is adjusted to fix the filling fraction, which we assume as  $n = 0.5$  here. We consider the S lattice to bear the size  $N_z \times N_y$  with periodic boundary conditions along  $z$  [Fig. 1(a)]. As we consider ideal insulating antiferromagnets, their thicknesses do not influence the phenomena investigated here.

A local spin-splitting field  $J\mathbf{M}_j/2$  is imposed by the two AFIs onto the S interfacial monolayers  $(j_z, 1)$  and  $(j_z, N_y)$ . Here,  $J$  parametrizes the AFI-S interfacial exchange coupling. As depicted in Fig. 1(a), the magnetic moments in the first AFI have a fixed orientation corresponding to the Néel vector  $\mathbf{n}_1 = \mathbf{z}$  so that  $\mathbf{M}_{(j_z,1)} = (-1)^{j_z-1} \mathbf{n}_1$ . The Néel vector  $\mathbf{n}_2 = [\cos(\theta)\mathbf{z} + \sin(\theta)\mathbf{y}]$  of the second AFI leads to rotation of the local spin-splitting oriented along  $\mathbf{M}_{(j_z,N_y)} = (-1)^{j_z-1} \mathbf{n}_2$ .

We numerically diagonalize the Hamiltonian in Eq. (1) by solving the Bogoliubov-de Gennes equation [42] self-consistently:

$$H = H_0 + \sum_n' E_n \gamma_n^\dagger \gamma_n \quad \text{with} \quad (2)$$

$$H_0 = -N\mu - \sum_j \frac{|\Delta_j|^2}{U} - \frac{1}{2} \sum_n' E_n, \quad (3)$$

where  $\sum_n'$  denotes the sum over positive eigenenergies  $E_n > 0$  only,  $\{\gamma_n^\dagger\}$  is a set of unique fermion operators, and  $N = N_z N_y$  is the total number of S lattice sites. The resulting solution provides complete information on the superconducting or normal state of the S layer.

## III. CRITICAL TEMPERATURE CONTROL VIA $\theta$

In order to examine the magnetoresistance and S layer's critical temperature dependence on the AFIs, we numerically compute the superconducting critical temperature  $T_c$ . It is determined using a binary search algorithm locating the temperature at which the superconducting gap starts to increase from a near-zero initial guess upon its self-consistent evaluation [43, 44].

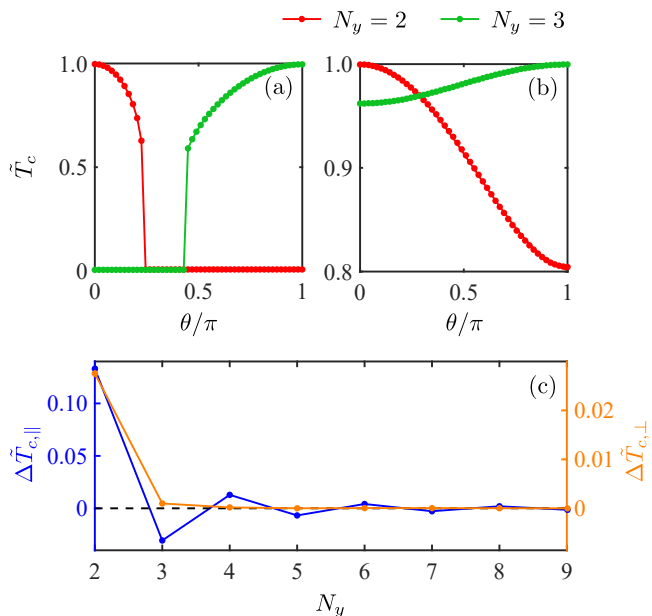


FIG. 2. Normalized critical temperature  $\tilde{T}_c$  variation with  $\theta$  for (a) stronger and (b) weaker interfacial exchange coupling  $J$ . The variation is reversed when the number of S monolayers  $N_y$  changes from even to odd. A complete suppression of  $T_c$  is observed for the stronger  $J$  case (a), while the weaker exchange (b) results in variation of  $T_c$  as per Eq. (4). (c) By fitting the numerically evaluated  $\tilde{T}_c(\theta)$  to Eq. (4) for different thicknesses  $N_y$ ,  $\Delta\tilde{T}_{c,\parallel}$  and  $\Delta\tilde{T}_{c,\perp}$  are obtained and studied for their thickness  $N_y$  dependence. The parity effect of  $\Delta\tilde{T}_{c,\parallel}$  with respect to  $N_y$  results from the alternating sign of Néel triplets' amplitude, as discussed in Fig. 1. In all panels,  $N_z = 202$ . In (a),  $U/t = 1$  and  $J/t = 0.08$ . In (b),  $U/t = 1$  and  $J/t = 0.02$ . In (c),  $U/t = 1.3$  and  $J/t = 0.08$ .

To succinctly capture and present the  $T_c$  variation with  $\theta$  for different thicknesses  $N_y$  of the S layer, we first parametrize  $T_c$  vs.  $\theta$  on symmetry grounds. This parametrization is only valid for small changes in  $T_c$ . For a small  $J$ ,  $T_c$  is only weakly altered by the adjacent AFIs and is expected to bear the dependence:

$$\tilde{T}_c(\theta) \equiv \frac{T_c(\theta)}{T_{c,0}} \equiv \Delta\tilde{T}_{c,\parallel} \cos\theta + \Delta\tilde{T}_{c,\perp} \sin^2\theta + \tilde{T}_{c,\parallel}, \quad (4)$$

where  $T_{c,0}$  is the critical temperature of the same S layer when it is not coupled to the AFIs, i.e., assuming  $J = 0$  in Eq. (1). From Eq. (4) above, we see that

$$\begin{aligned} \Delta\tilde{T}_{c,\parallel} &= [\tilde{T}_c(0) - \tilde{T}_c(\pi)]/2, & \tilde{T}_{c,\parallel} &= [\tilde{T}_c(0) + \tilde{T}_c(\pi)]/2, \\ \Delta\tilde{T}_{c,\perp} &= \tilde{T}_c(\pi/2) - \tilde{T}_{c,\parallel}. \end{aligned} \quad (5)$$

In Eq. (4), the  $\Delta\tilde{T}_{c,\parallel} \cos\theta$  term is expected due to the interference of zero-spin Néel triplets generated by the two AFI-S interfaces [37], as briefly outlined in Fig. 1. It is analogous to the  $\cos\theta$  dependence in F-S-F trilayers [11, 12] and bears the symmetry of vectorial addition of the spin-splitting fields from the two AFIs.

The  $\Delta\tilde{T}_{c,\perp} \sin^2\theta$  term is expected from the generation of equal-spin triplets via the noncollinearity between  $\mathbf{n}_1$  and  $\mathbf{n}_2$  [38–41] as it is finite only when the two magnetic orders are noncollinear. In Eq. (4),  $\Delta\tilde{T}_{c,\parallel}$  characterizes the  $T_c$  difference between parallel and antiparallel configurations. When it is positive (negative), the  $T_c$  is larger for the parallel (antiparallel) configuration of the magnetic orders. On the other hand,  $\Delta\tilde{T}_{c,\perp}$  represents the change in  $T_c$  when going from parallel to perpendicular configurations. Together,  $\Delta\tilde{T}_{c,\parallel}$  and  $\Delta\tilde{T}_{c,\perp}$  provide a succinct parametrization to study and present  $T_c$  vs.  $\theta$  in our system. We emphasize that our numerical evaluation of  $T_c$  does not depend on or assume this parametrization [Eq. (4)].

In Fig. 2(a), we depict the  $\tilde{T}_c$  variation when the interfacial exchange is strong and results in a complete  $T_c$  suppression for certain  $\theta$ . When the number of S monolayers  $N_y = 2$ , the Néel triplets generated by the two AFI-S interfaces interfere destructively for  $\theta = 0$ . This results in a weakening of the effect due to the AFIs and a larger  $T_c$  at  $\theta = 0$ . For  $N_y = 3$ , the interference becomes constructive for  $\theta = 0$  [Fig. 1(c)] due to the checkerboard pattern of the Néel triplets [Fig. 1(b)] and the  $T_c$  vs.  $\theta$  trend is reversed. When the exchange coupling  $J$  is small enough to avoid a complete suppression of  $T_c$ , the numerically evaluated  $\tilde{T}_c(\theta)$  [Fig. 2(b)] is found to perfectly fit Eq. (4). The reversal of trends between  $N_y = 2$  and 3 remains as before and is attributed to the interference and checkerboard effects.

Considering a filling fraction  $n = 0.6$ , we found a negligible dependence of  $T_c$  on  $\theta$ . This is consistent with a much weaker generation of Néel triplets away from  $n = 0.5$  corresponding to  $\mu = 0$  [41]. Furthermore, for a direct comparison, we discuss plots analogous to Figs. 2(a) and (b) for a trilayer comprising ferromagnetic insulator (FI) instead of AFI in the Appendix. The FI-S-FI trilayer is found to exhibit a weaker  $T_c$  dependence, lack of an abrupt jump to 0 seen in Fig. 2(a), and no reversal of  $T_c$  variation between  $N_y = 2$  and 3. This emphasizes the several unique features of our investigated AFI-S-AFI system. Here, we have considered AFIs with zero net magnetic moments. In the presence of a finite magnetic moment due to canting [41], we expect the  $T_c$  variation to bear a small contribution reminiscent of the FI-S-FI case investigated in the Appendix.

Finally, Fig. 3(c) shows the dependence of  $\Delta\tilde{T}_{c,\parallel}$  and  $\Delta\tilde{T}_{c,\perp}$  on  $N_y$  obtained by fitting the numerically evaluated data to Eq. (4).  $\Delta\tilde{T}_{c,\parallel}$ , found to be an order of magnitude larger than  $\Delta\tilde{T}_{c,\perp}$ , exhibits a parity effect with  $N_y$  due to the checkerboard pattern of Néel triplets [Fig. 1(b)] and the resulting interference effects [Figs. 1(c) and (d)]. This further validates the argument presented above that the  $\Delta\tilde{T}_{c,\parallel} \cos\theta$  term stems from the Néel zero-spin triplets [37, 41]. As  $\Delta\tilde{T}_{c,\perp}$  stems from the regular equal-spin triplets generated by the noncollinearity between  $\mathbf{n}_1$  and  $\mathbf{n}_2$  [38–40], it exhibits a simple decay with  $N_y$  without any alternation of its sign.

The results presented above (Fig. 2) show that an infinite magnetoresistance [18], resulting from a switching between the normal resistive and superconducting states using an applied magnetic field, is achievable in the considered AFI–S–AFI trilayer by reorienting the Néel vector of one AFI with respect to the other. Recent experiments already demonstrate manipulation of the Néel vector in an easy-plane AFI, such as hematite above the Morin transition [45], using small magnetic fields [46]. Furthermore, a complete suppression of  $T_c$  [Fig. 1(a)] enables such a device at arbitrarily low temperatures. An observation of the parity effect with  $N_y$  [Fig. 2(c)] will additionally provide evidence in favor of these recently predicted Néel triplets.

#### IV. NÉEL TRIPLETS-MEDIATED COUPLING BETWEEN THE ANTIFERROMAGNETIC INSULATORS

We have learned above how generation of Néel triplets by the two AFIs enables control over the superconducting state in an AFI–S–AFI trilayer. Now, we seek to examine the inverse effect i.e., how the superconducting condensate enables a coupling between the two Néel vectors  $\mathbf{n}_1$  and  $\mathbf{n}_2$  [Fig. 3(a)]. This is distinct from the conventional exchange coupling between two magnetizations [11]. Since the latter vanishes in a typical AFI, coupling two AFIs is more challenging and rewarding. Furthermore, in an FI–S–FI trilayer, the coupling between the two magnetic orders mediated by Cooper pairs competes with a direct dipolar interaction between them. A lack of the latter in our AFI–S–AFI system makes the role of Cooper pairs more important.

To examine the desired coupling, we need to compute the S layer free energy density  $f$  as a function of  $\theta$ . It is given by  $f = -(1/\beta N)\ln(Z)$ , where the partition function  $Z$  is  $Z = \text{Tr}[\exp(-\beta H)]$ . Here,  $\beta = 1/k_B T$  with  $k_B$  the Boltzmann constant and  $T$  the temperature. Inserting the diagonalized Hamiltonian Eq. (2) into the free energy density expression above, we obtain

$$f = \frac{H_0}{N} - \frac{1}{\beta N} \sum_n \ln(1 + e^{-\beta E_n}), \quad (6)$$

which is evaluated numerically [36]. This free energy density [Eq. (6)] includes the contribution of quasiparticles, which can also mediate a coupling between the two AFIs [21, 47–49]. Since we are interested in the superconducting condensate's role in mediating this coupling, we focus on the superconducting condensation energy density contribution:  $f_C \equiv f_N - f_S$  attributed to the Cooper pairs [50]. Here,  $f_N$  ( $f_S$ ) denotes the free energy density in the normal (superconducting) state and is obtained when  $U = 0$  ( $U \neq 0$ ) in the Hamiltonian Eq. (1).

Making symmetry-based and physical arguments similar to the ones put forward in assuming the  $T_c$  depen-

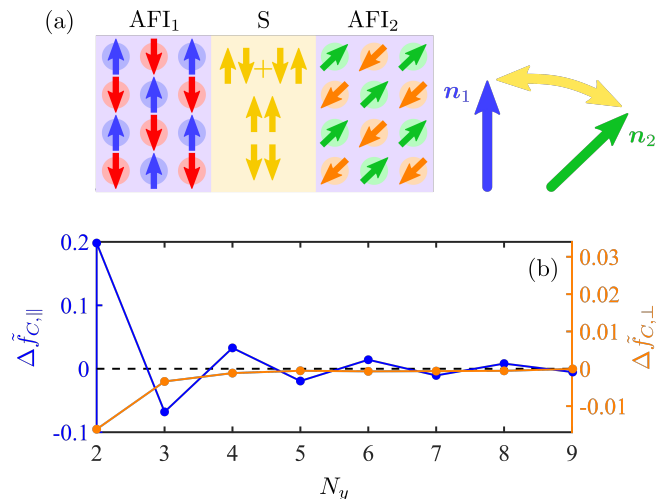


FIG. 3. (a) Spin-triplet Cooper pairs generated by the AFIs mediate coupling between the two Néel vectors  $\mathbf{n}_1$  and  $\mathbf{n}_2$ . This coupling is captured by the superconducting condensate's contribution  $f_C$  to the  $\theta$ -dependence of the free energy density. (b) Fitting numerically evaluated  $f_C$  to Eq. (7) yields  $\Delta \tilde{f}_{C,\parallel}$  and  $\Delta \tilde{f}_{C,\perp}$ , which are plotted vs.  $N_y$  thereby delineating the thickness dependence of the mediated coupling. We have employed  $N_z = 202$ ,  $U/t = 1.3$ ,  $J/t = 0.05$ , and  $\beta t = 10^4$ .

dence Eq. (4), we expect the relation

$$\tilde{f}_C(\theta) \equiv \frac{f_C(\theta)}{f_{C,0}} \equiv \Delta \tilde{f}_{C,\parallel} (\mathbf{n}_1 \cdot \mathbf{n}_2) + \Delta \tilde{f}_{C,\perp} (\mathbf{n}_1 \times \mathbf{n}_2)^2 + \tilde{f}_{c,\parallel}, \quad (7)$$

where  $f_{C,0}$  is the condensation energy for the same S layer without the adjacent AFIs i.e., considering  $J = 0$  in Eq. (1). Furthermore, we have expressed  $\theta$  in terms of the Néel unit vectors to emphasize and clarify their mutual coupling [Fig. 3(a)].

Evaluating  $\tilde{f}_C(\theta)$  numerically, we find the results to fit Eq. (7) perfectly thereby vindicating it and providing the desired  $\Delta \tilde{f}_{C,\parallel}$  and  $\Delta \tilde{f}_{C,\perp}$ . These have been plotted in Fig. 3(b) for different number  $N_y$  of S monolayers.  $\Delta \tilde{f}_{C,\parallel}$  originates from the Néel zero-spin triplets [37, 41] and captures an exchange-like interaction between the two AFIs' Néel orders. Consequently, it also bears the parity effect resulting from the alternating nature of the pairing amplitude [Fig. 1(b)]. On the other hand,  $\Delta \tilde{f}_{C,\perp}$  represents an unconventional interaction originating from the equal-spin triplets induced by the noncollinearity between  $\mathbf{n}_1$  and  $\mathbf{n}_2$ .

Altogether, Fig. 3 delineates the thickness dependence of the desired coupling between the two AFIs' Néel orders, which may find applications in control over AFIs. At the same time, the similarity between Figs. 2(c) and 3(b) indicates the complementarity between and a common origin of the effects investigated here providing valuable insights into the Néel proximity effect and Cooper pairs.

## V. CONCLUSION

Employing the Bogoliubov-de Gennes framework and numerical diagonalization of the Hamiltonian, we have demonstrated a control of the superconducting critical temperature ( $T_c$ ) and a condensate-mediated coupling between the two Néel vectors in an AFI-S-AFI trilayer with compensated interfaces. Our investigated trilayer manifests various advantages over its conventional FI-S-FI counterpart including a stronger effect on  $T_c$  and no interference from magnetostatic fields in the coupling between the two magnetic orders. The demonstrated dependence of  $T_c$  on the two Néel vectors enables an infinite magnetoresistance in the current-in-plane geometry via switching between the normal and superconducting states of the S layer [18]. An interference between the spin-triplet Cooper pairs generated by the AFI-S interfaces is further shown to enable coupling between the two AFIs' Néel vectors  $\mathbf{n}_1$  and  $\mathbf{n}_2$ . The predominant coupling mediated by the Néel zero-spin triplets is exchange-like  $\sim \mathbf{n}_1 \cdot \mathbf{n}_2$ , while a weaker coupling of the form  $\sim (\mathbf{n}_1 \times \mathbf{n}_2)^2$  is caused by equal-spin triplets. These phenomena are enabled by the recently predicted Néel triplet Cooper pairs [37] generated at such compensated AFI-S interfaces. As a result they bear a distinct parity effect carrying signatures of the Néel triplets' alternating amplitude and should provide the means to experimentally observe them. Thus, our work paves the way for investigating a broad range of superconducting hybrids incorporating antiferromagnets including the effects of spin-orbit coupling. At the same time, the phenomena discussed here outline possibilities for exploiting the broad range of advantages offered by antiferromagnets in superconducting spintronic devices and phenomena.

## ACKNOWLEDGMENTS

S.C. and A.K. acknowledge financial support from the Spanish Ministry for Science and Innovation – AEI Grant CEX2018-000805-M (through the “Maria de Maeztu” Programme for Units of Excellence in R&D) and grant RYC2021-031063-I funded by MCIN/AEI/10.13039/501100011033 and “European Union Next Generation EU/PRTR”. L.J.K. acknowledges financial support from the Research Council of Norway through its Centers of Excellence funding scheme, project 262633, “QuSpin”. I.V.B., G.A.B. and V.M.G. acknowledge support from MIPT, Project FSMG-2023-0014.

### Appendix A:

#### Ferromagnet-superconductor-ferromagnet trilayer

Here, we consider trilayers comprised by ferromagnetic insulator (FI) layers [see Fig. 4(a)] instead of the compensated antiferromagnetic insulator (AFI) layers con-

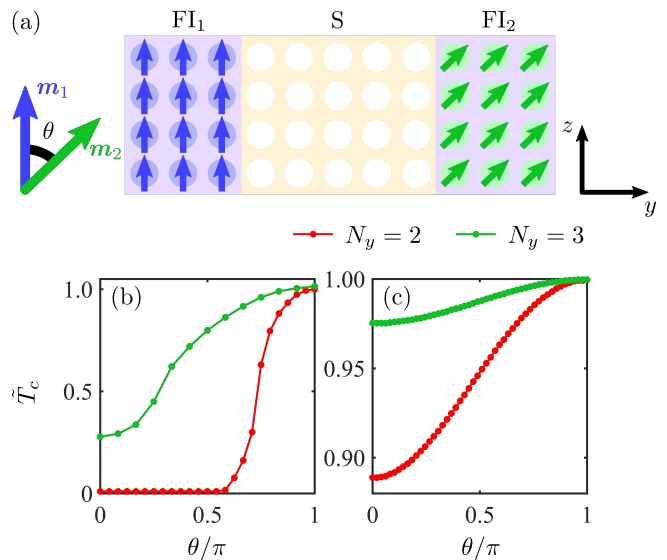


FIG. 4. (a) Schematic depiction of a system where the compensated AFIs are replaced with ferromagnetic insulators (FIs) with magnetization along  $\mathbf{m}_1$  and  $\mathbf{m}_2$  that subtend an angle  $\theta$ . The normalized critical temperature  $\tilde{T}_c$  variation with  $\theta$  is plotted for (b) stronger and (c) weaker interfacial exchange coupling  $J$ . Contrary to the AFI/S/AFI system, the variation is no longer reversed when the number of S monolayers  $N_y$  changes from even to odd. The weaker exchange (b) results in variation of  $T_c$  as per Eq. (4) in the main text. In both panels,  $N_z = 402$  and  $U/t = 1$ . In (b),  $J/t = 0.08$ . In (c),  $J/t = 0.02$ .

sidered in the main text. Employing the same numerical routines, we evaluate  $T_c$  as a function of the angle  $\theta$  between magnetic orders of the two FI layers. The plots in Figs. 4(b) and (c) show data analogous to that in Figs. 2(a) and (b) of the main text, including use of the same parameter values.

There are two minor differences in the numerical method though. First, we needed to employ a larger value of  $N_z$  to adequately capture the superconducting properties. This is because the density of states for the AFI-S-AFI is larger than its FI-S-FI counterpart for the considered parameters. Thus, a larger number of lattice sites was needed to obtain convergent values for the FI-S-FI trilayer. Secondly, the algorithm for  $T_c$  evaluation needs to be modified and in each binary search iteration, the superconducting gap needs to be established self-consistently. This is because the FI-S-FI system manifests a first-order phase transition with temperature [9, 10] for larger values of  $J$ . There are thus multiple stable solutions for the superconducting state for a range of parameters. Our updated  $T_c$  search algorithm overcomes all these complications. As a result, the numerical evaluation for the FI-S-FI system was much more computationally intensive, resulting in our providing fewer data points in Fig. 4(b).

The numerically evaluated data plotted in Figs. 4(b) and (c) shows that the variation of  $T_c$  is weaker in the

case of FI-S-FI, as compared to the situation in AFI-S-AFI. Furthermore, the maximum  $T_c$  is always obtained at  $\theta = \pi$ , as expected [11]. There is no parity effect with the number of S layers, reinforcing our argument that the observed parity effect in AFI-S-AFI system is

a smoking gun signature of the Néel triplets. Finally, Fig. 4(b) shows that for the FI-S-FI system,  $T_c$  varies smoothly with  $\theta$  and there is no abrupt jump to 0, like what is seen for the AFI-S-AFI case.

- 
- [1] M. Sigrist and K. Ueda, Phenomenological theory of unconventional superconductivity, *Rev. Mod. Phys.* **63**, 239 (1991).
- [2] A. I. Buzdin, Proximity effects in superconductor-ferromagnet heterostructures, *Rev. Mod. Phys.* **77**, 935 (2005).
- [3] F. S. Bergeret, A. F. Volkov, and K. B. Efetov, Odd triplet superconductivity and related phenomena in superconductor-ferromagnet structures, *Rev. Mod. Phys.* **77**, 1321 (2005).
- [4] Y. Tanaka, M. Sato, and N. Nagaosa, Symmetry and topology in superconductors –odd-frequency pairing and edge states–, *Journal of the Physical Society of Japan* **81**, 011013 (2012).
- [5] M. Eschrig, Spin-polarized supercurrents for spintronics: a review of current progress, *Reports On Progress In Physics* **78**, 104501 (2015).
- [6] J. Linder and J. W. A. Robinson, Superconducting spintronics, *Nature Physics* **11**, 307 (2015).
- [7] F. S. Bergeret, M. Silaev, P. Virtanen, and T. T. Heikkilä, Colloquium: Nonequilibrium effects in superconductors with a spin-splitting field, *Rev. Mod. Phys.* **90**, 041001 (2018).
- [8] K. Maki and T. Tsuneto, Pauli paramagnetism and superconducting state, *Progress of Theoretical Physics* **31**, 945 (1964).
- [9] A. M. Clogston, Upper limit for the critical field in hard superconductors, *Phys. Rev. Lett.* **9**, 266 (1962).
- [10] B. S. Chandrasekhar, A note on the maximum critical field of high-field superconductors, *Applied Physics Letters* **1**, 7 (1962).
- [11] P. De Gennes, Coupling between ferromagnets through a superconducting layer, *Physics Letters* **23**, 10 (1966).
- [12] G. Deutscher and F. Meunier, Coupling between ferromagnetic layers through a superconductor, *Phys. Rev. Lett.* **22**, 395 (1969).
- [13] L. R. Tagirov, Low-field superconducting spin switch based on a superconductor /ferromagnet multilayer, *Phys. Rev. Lett.* **83**, 2058 (1999).
- [14] M. L. Kulić and M. Endres, Ferromagnetic-semiconductor-singlet-(or triplet) superconductor-ferromagnetic-semiconductor systems as possible logic circuits and switches, *Phys. Rev. B* **62**, 11846 (2000).
- [15] J. Y. Gu, C.-Y. You, J. S. Jiang, J. Pearson, Y. B. Bazaliy, and S. D. Bader, Magnetization-orientation dependence of the superconducting transition temperature in the ferromagnet-superconductor-ferromagnet system: CuNi/Nb/CuNi, *Phys. Rev. Lett.* **89**, 267001 (2002).
- [16] K. Westerholt, D. Sprungmann, H. Zabel, R. Brucas, B. Hjörvarsson, D. A. Tikhonov, and I. A. Garifullin, Superconducting spin valve effect of a v layer coupled to an antiferromagnetic [Fe/V] superlattice, *Phys. Rev. Lett.* **95**, 097003 (2005).
- [17] I. C. Moraru, W. P. Pratt, and N. O. Birge, Magnetization-dependent  $T_c$  shift in ferromagnet/superconductor/ferromagnet trilayers with a strong ferromagnet, *Phys. Rev. Lett.* **96**, 037004 (2006).
- [18] B. Li, N. Roschewsky, B. A. Assaf, M. Eich, M. Epstein-Martin, D. Heiman, M. Münzenberg, and J. S. Moodera, Superconducting spin switch with infinite magnetoresistance induced by an internal exchange field, *Phys. Rev. Lett.* **110**, 097001 (2013).
- [19] Y. Gu, G. B. Halász, J. W. A. Robinson, and M. G. Blamire, Large superconducting spin valve effect and ultrasmall exchange splitting in epitaxial rare-earth-niobium trilayers, *Phys. Rev. Lett.* **115**, 067201 (2015).
- [20] E. V. Gomonay and V. M. Loktev, Spintronics of antiferromagnetic systems (review article), *Low Temperature Physics* **40**, 17 (2014).
- [21] V. Baltz, A. Manchon, M. Tsoi, T. Moriyama, T. Ono, and Y. Tserkovnyak, Antiferromagnetic spintronics, *Rev. Mod. Phys.* **90**, 015005 (2018).
- [22] T. Jungwirth, X. Marti, P. Wadley, and J. Wunderlich, Antiferromagnetic spintronics, *Nature Nanotechnology* **11**, 231 (2016).
- [23] A. Kamra, A. Rezaei, and W. Belzig, Spin splitting induced in a superconductor by an antiferromagnetic insulator, *Phys. Rev. Lett.* **121**, 247702 (2018).
- [24] L. Šmejkal, Y. Mokrousov, B. Yan, and A. H. MacDonald, Topological antiferromagnetic spintronics, *Nature Physics* **14**, 242 (2018).
- [25] J. J. Hauser, H. C. Theuerer, and N. R. Werthamer, Proximity effects between superconducting and magnetic films, *Phys. Rev.* **142**, 118 (1966).
- [26] I. V. Bobkova, P. J. Hirschfeld, and Y. S. Barash, Spin-dependent quasiparticle reflection and bound states at interfaces with itinerant antiferromagnets, *Phys. Rev. Lett.* **94**, 037005 (2005).
- [27] B. M. Andersen, I. V. Bobkova, P. J. Hirschfeld, and Y. S. Barash, Bound states at the interface between antiferromagnets and superconductors, *Phys. Rev. B* **72**, 184510 (2005).
- [28] B. M. Andersen, I. V. Bobkova, P. J. Hirschfeld, and Y. S. Barash,  $0 - \pi$  transitions in josephson junctions with antiferromagnetic interlayers, *Phys. Rev. Lett.* **96**, 117005 (2006).
- [29] M. F. Jakobsen, K. B. Naess, P. Dutta, A. Brataas, and A. Qaiumzadeh, Electrical and thermal transport in antiferromagnet-superconductor junctions, *Phys. Rev. B* **102**, 140504 (2020).
- [30] M. Hübener, D. Tikhonov, I. A. Garifullin, K. Westerholt, and H. Zabel, The antiferromagnet/superconductor proximity effect in Cr/V/Cr trilayers, *Journal Of Physics-Condensed Matter* **14**, 8687 (2002).
- [31] C. Bell, E. J. Tarte, G. Burnell, C. W. Leung, D.-J. Kang, and M. G. Blamire, Proximity and josephson effects in superconductor/antiferromagnetic Nb/ $\gamma$ -Fe<sub>50</sub>Mn<sub>50</sub> heterostructures, *Phys. Rev. B* **68**, 144517 (2003).

- [32] B. L. Wu, Y. M. Yang, Z. B. Guo, Y. H. Wu, and J. J. Qiu, Suppression of superconductivity in Nb by IrMn in IrMn/Nb bilayers, *Applied Physics Letters* **103**, 152602 (2013).
- [33] R. L. Seeger, G. Forestier, O. Gladii, M. Leiviskä, S. Auffret, I. Joumard, C. Gomez, M. Rubio-Roy, A. I. Buzdin, M. Houzet, and V. Baltz, Penetration depth of cooper pairs in the IrMn antiferromagnet, *Phys. Rev. B* **104**, 054413 (2021).
- [34] A. Mani, T. G. Kumary, D. Hsu, J. G. Lin, and C.-H. Chern, Modulation of superconductivity by spin canting in a hybrid antiferromagnet/superconductor oxide, *Applied Physics Letters* **94**, 072509 (2009).
- [35] A. Mani, T. G. Kumary, and J. G. Lin, Thickness controlled proximity effects in c-type antiferromagnet/superconductor heterostructure, *Scientific Reports* **5**, 12780 (2015).
- [36] L. G. Johnsen, S. H. Jacobsen, and J. Linder, Magnetic control of superconducting heterostructures using compensated antiferromagnets, *Phys. Rev. B* **103**, L060505 (2021).
- [37] G. A. Bobkov, I. V. Bobkova, A. M. Bobkov, and A. Kamra, Néel proximity effect at antiferromagnet/superconductor interfaces, *Phys. Rev. B* **106**, 144512 (2022).
- [38] A. F. Volkov, F. S. Bergeret, and K. B. Efetov, Odd triplet superconductivity in superconductor-ferromagnet multilayered structures, *Phys. Rev. Lett.* **90**, 117006 (2003).
- [39] Y. V. Fominov, A. A. Golubov, T. Y. Karinskaya, M. Y. Kupriyanov, R. G. Deminov, and L. R. Tagirov, Superconducting triplet spin valve, *JETP Letters* **91**, 308 (2010).
- [40] P. V. Leksin, N. N. Garif'yanov, I. A. Garifullin, Y. V. Fominov, J. Schumann, Y. Krupskaya, V. Kataev, O. G. Schmidt, and B. Büchner, Evidence for triplet superconductivity in a superconductor-ferromagnet spin valve, *Phys. Rev. Lett.* **109**, 057005 (2012).
- [41] S. Chourasia, L. J. Kamra, I. V. Bobkova, and A. Kamra, Generation of spin-triplet cooper pairs via a canted antiferromagnet, *Phys. Rev. B* **108**, 064515 (2023).
- [42] J. Zhu, *Bogoliubov-de Gennes Method and Its Applications*, Lecture Notes in Physics (Springer International Publishing, 2016).
- [43] L. G. Johnsen, N. Banerjee, and J. Linder, Magnetization reorientation due to the superconducting transition in heavy-metal heterostructures, *Phys. Rev. B* **99**, 134516 (2019).
- [44] L. G. Johnsen, K. Svalland, and J. Linder, Controlling the superconducting transition by rotation of an inversion symmetry-breaking axis, *Phys. Rev. Lett.* **125**, 107002 (2020).
- [45] A. H. Morrish, *Canted Antiferromagnetism: Hematite* (WORLD SCIENTIFIC, 1995).
- [46] T. Wimmer, A. Kamra, J. Gückelhorn, M. Opel, S. Geprägs, R. Gross, H. Huebl, and M. Althammer, Observation of antiferromagnetic magnon pseudospin dynamics and the Hanle effect, *Phys. Rev. Lett.* **125**, 247204 (2020).
- [47] A. S. Núñez, R. A. Duine, P. Haney, and A. H. MacDonald, Theory of spin torques and giant magnetoresistance in antiferromagnetic metals, *Phys. Rev. B* **73**, 214426 (2006).
- [48] P. M. Haney, D. Waldron, R. A. Duine, A. S. Núñez, H. Guo, and A. H. MacDonald, Ab initio giant magnetoresistance and current-induced torques in Cr/Au/Cr multilayers, *Phys. Rev. B* **75**, 174428 (2007).
- [49] Y. Xu, S. Wang, and K. Xia, Spin-transfer torques in antiferromagnetic metals from first principles, *Phys. Rev. Lett.* **100**, 226602 (2008).
- [50] P. De Gennes, *Superconductivity Of Metals And Alloys* (CRC Press, 2018).